Femtosecond laser-assisted selective holding with ultra-low power for direct manipulation of biological species

Krishangi Krishna [iD],[a] Joshua A. Burrow [iD],[a] Zhaowei Jiang [iD],[b] Wenyu Liu [iD],[a] Anita Shukla,[b] and Kimani C. Toussaint Jr.[a,c,*]

[a]Brown University, School of Engineering, PROBE Lab, Providence, Rhode Island, United States
[b]Brown University, School of Engineering, Shukla Lab, Providence, Rhode Island, United States
[c]Brown–Lifespan Center for Digital Health, Providence, Rhode Island, United States

ABSTRACT.   **Significance:** Optical tweezers (OTs) have emerged as an essential technique for manipulating nanoscopic particulates and biological specimens with sub-micron precision and have revolutionized various fields, including biology and colloidal physics. However, traditional optical trapping techniques often rely on moderate- to high-power continuous wave (CW) lasers, which can introduce unwanted thermal effects and photodamage to delicate samples. An innovative alternative has emerged through the utilization of femtosecond (fs) lasers at ultra-low average powers on the order of tens of microwatt. Unexpectedly overlooked until now, this method enables the direct trapping and manipulation of cells without relying on functionalized spheres.

Aim: We aim to compare the trap stiffness of CW and fs lasers in an unexplored average power regime (sub-1 mW) on cells within the intermediate-size regime.

Approach: A CW or fs laser is used to trap cells in an inverted microscope setup. We trap five different pathogenic bacteria with different morphologies to compare trap stiffness.

Results: We find that fs laser-assisted selective holding with ultra-low power (FLASH-UP) exhibits five times greater trap stiffness than CW-based OTs and can trap at lower intensities. Furthermore, we demonstrate that FLASH-UP does not impact cell motility.

Conclusions: FLASH-UP displays higher trap stiffness at average powers below 1 mW and does not impact cell functionality. These results pave the way for ultra-low-power trapping of cells for applications in sorting, bio-sensing, *in vivo* cell manipulation, and single-cell analysis.

1 Introduction

Optical tweezers (OTs), originally conceptualized by Arthur Ashkin in the 1970s,[1–3] remain a valuable, non-invasive tool for cellular manipulation ranging from individual to populations of cells in aqueous environments.[4–6] Specifically, OT has been used for cell sorting,[7] live cell patterning,[8] single-cell optoporation and transfection,[9] and characterizing the mechanical properties

---

*Address all correspondence to Kimani C. Toussaint, Jr., kimani_toussaint@brown.edu

of cells in different growth media,[10] collagen,[11] and DNA.[12] OT is a result of balancing the electromagnetic gradient and scattering forces in a trap, a phenomenon that is a consequence of light's radiation pressure. The net force acting on a particle caught in an optical trap is on the order of piconewtons, which is on the same scale as forces produced by the naturally occurring mechanoenzymes in biology.[4,13,14] A typical OT setup is constructed from an inverted, laser-scanning optical microscope, whereby a single-wavelength, continuous wave (CW) laser source delivering powers in the range of 5 to 100 mW (corresponding to intensities of ~22 to 77.5 MW/cm^2) for strong, diffraction-limited focusing is employed.[15–18] For specific applications for biological manipulation, optical wavelengths in the near-infrared regime and intensities on the order of MW/cm^2 are used.[4,6,19]

The laser-induced heating resulting from light absorption in the cell cytosol causes thermal damage to the trapped biological specimens and the generation of toxic reactive oxygen species.[14,20,21] Researchers have explored various methods to mitigate this issue such as reducing the total heat generated by trapping at $T = 0°C$,[22,23] minimizing the duration that trapped cells are exposed to the laser,[14,21] and relying on indirect trapping methods that involve tweezing dielectric particles that are tethered to the biological species of interest.[10,24,25] Nonetheless, these alternate methods limit the ability to directly interrogate cell–cell interactions. In the specific case of trapping bacteria, it has been shown that the local heating results in adverse effects that impact their propagation, motility, and expression of stress-response genes, even when exposed to the minimal threshold intensities required for trapping.[20,26] Importantly, these traditional cases of OT for biological manipulation use CW lasers. An alternative approach has stemmed from the use of ultrafast, femtosecond (fs)-pulsed lasers operating at megahertz (MHz) repetition rates, in which the high peak powers and short pulse durations result in nanojoule pulse energies that are less deleterious to cells.[27,28]

In the Rayleigh regime (for particles of diameter $d <$ wavelength of light λ), fs-OT indirectly trapped DNA by being tethered to a micron-sized dielectric particle.[27] The merits of employing fs-OT over one that is CW have been exemplified for this regime in which fs-OT trapped particles with average powers an order of magnitude lower than that required for CW. Due to the particle size, there is an increase in thermal diffusion, which is offset by the ultra-high peak powers of pulsed lasers with the generation of transient forces.[29,30] In the Lorenz–Mie ($d \approx \lambda$) and Mie ($d > \lambda$) regimes, fs-OT directly trapped bacteria such as *Escherichia coli*, eukaryotic cells such as *Phaffia rhodozyma*, and red blood cells. However, the power densities used to trap these cells led to cell membrane dysfunction and the formation of damaged white spots after being trapped for 1 to 15 min.[26,28,31] Interestingly, investigations into trap efficiency for particles in the intermediate regime have yielded conflicting results between CW and fs sources. Agate et al.[32] concluded that stiffness is determined by average power rather than peak power. However, Singh et al.[33] presented contrasting findings, demonstrating a notable distinction in extrapolated corner frequencies, with pulsed lasers exhibiting superior performance over the CW source. Notably, these investigations were conducted using input laser powers on the order of 5 to 100 mW. However, there has been limited exploration of OT efficiency at average powers sub-1 mW for particles existing within the Lorenz–Mie regime, a domain highly pertinent to cellular studies.

In this work, we demonstrate fs laser-assisted selective holding with ultra-low power (FLASH-UP) to achieve optical tweezing of dielectrics using average powers deep in the microwatt for objects in the Lorenz–Mie regime. This technique is readily applicable to the OT community as the standard OT setup is used with the substitution of the CW source for an fs pulsed source. We apply FLASH-UP to pathogenic bacterial cells with pili, including *Staphylococcus aureus*, *Bacillus paranthracis*, *Vibrio cholerae*, and *Staphylococcus epidermidis*. Last, we tweeze *Pseudomonas aeruginosa*, an infectious bacteria species with a single polar flagellum moving with a speed of 50 μm/s that often causes pneumonia or leads to bacteremia. We find that FLASH-UP demonstrates a trap stiffness 5× greater than CW-OT for dielectric spheres and can trap at power densities half that of CW. To a first approximation, the use of an ultrafast source introduces a transient force component that works in concert with the traditional gradient force to achieve stable optical trapping. The implications of these results will allow for the characterization of bacteria on a single-cell level, offering insights into mechanistic clues hidden in bulk measurements and a stronger understanding of pathogenic mechanisms.[34]

2 Theory

The modeling of fs OT in the Lorenz–Mie regime is the subject of work that we are currently pursuing and will be reported elsewhere. Nonetheless, valuable insights can be obtained from examining the effects of the Rayleigh model. The time-varying electric field E of a Gaussian beam propagating along the z-axis and polarized along $\hat{x}$ is expressed as[35]

$$\boldsymbol{E}(\rho, z, t) = \hat{x}\frac{iE_0}{i + 2z/kw_0^2}\exp\left[i\omega_0 t - ikz - \frac{i2\ kz\rho^2}{(kw_0^2)^2 + 4z^2} - \frac{kw_0^2\rho^2}{(kw_0^2)^2 + 4z^2}\right]\exp\left[-\frac{(t - \frac{z}{c})^2}{\tau^2}\right],$$

(1)

where w_0 is the beam waist at $z = 0$ and ρ, $k = \frac{2\pi}{\lambda}$, ω_0, t, and τ are the radial coordinate, wave number, carrier frequency, time, and pulse duration, respectively. The resultant Lorenzian force $\boldsymbol{F_p}$ arising from spatial inhomogeneous field distributions acting on a Rayleigh particle is given as

$$\boldsymbol{F_p}(\rho, z, t) = [\boldsymbol{p}(\rho, z, t) \cdot \nabla \boldsymbol{E}(\rho, z, t)] + [\partial_t \boldsymbol{p}(\rho, z, t)] \times \boldsymbol{B}(\rho, z, t) = \boldsymbol{F}_{\text{grad}} + \boldsymbol{F}_t,$$

(2)

where $\boldsymbol{p} = \alpha \boldsymbol{E}$ and $\boldsymbol{B}$ are the dipole moment and corresponding magnetic flux, respectively. Here, $\alpha = 4\pi n_m^2 \varepsilon_0 r^3 [\frac{m^2 - 1}{m^2 + 2}]$, and ε_0, r, and m are the vacuum dielectric permittivity, radius of the particle, and ratio of the refractive indices of particle n_p to medium n_m, respectively. The forces generated is thus decomposed into

$$\boldsymbol{F}_{\text{grad},\rho} = \frac{\xi\tilde{\rho}}{(1 + 4\tilde{z}^2)},$$

(3)

$$\boldsymbol{F}_{\text{grad},z} = \frac{2\xi\tilde{z}}{kw_0}\left[\frac{1 + 4\tilde{z}^2 - 2\tilde{p}^2}{(1 + 4\tilde{z}^2)^2}\right],$$

(4)

$$\boldsymbol{F}_t = \left[\frac{\tilde{z}kw_0^2}{c\tau} - \tilde{t}\right]\left[\frac{\xi w_0}{c\tau} - \frac{8\mu_0 I(\rho, z, t)}{\tau}\right],$$

(5)

where $(\tilde{p}, \tilde{z}, \tilde{t}) = (\rho/w_0, z/w_0, t/\tau)$ and $I(\rho, z, t)$ are the normalized temporal-spatial coordinates and intensity of the electric field, respectively, and $\xi = \frac{2\alpha I(\rho,z,t)}{n_m \varepsilon_0 cw_0}$. Thus, the use of an ultrafast optical pulse introduces an auxiliary force term given in Eq. (5), which would otherwise be zero when using a traditional CW source. We observe that the temporal force depends inversely on the pulse duration (Fig. 1).

Last, the scattering force, which pushes the particle along the axial direction, is given by $\boldsymbol{F}_{\text{scat}} = \hat{z}\frac{\sigma n_m}{c}I(\rho, z, t)$. Here, $\sigma = \frac{8\pi}{3}(kr)^4 r^2 [\frac{m^2 - 1}{m^2 + 2}]$ is the particle cross-section.

3 Experimental Setup

As a proof-of-concept demonstration, we first employ a conventional single-beam OT experimental setup, shown in Fig. 2(a), and compare the trap stiffness on 1-μm diameter silica microspheres using a 120-fs-pulsed with a repetition rate of 80 MHz (Spectra-Physics, InSight X3, Milpitas, California, United States) or a CW (Newport, LQC905-85E, Irvine, California, United States) laser source operating at a central wavelength of 905 nm, which can be accessed by a flip mirror. We employ a customized Olympus IX83 inverted microscope.

The laser source is spatially filtered and expanded to produce a TEM$_{00}$ Gaussian intensity profile. It passes through the linear polarizer and neutral density (ND) filter for power adjustment at the sample plane. The laser is directed onto a 2D galvanometer that controls the position of the laser. The laser is guided into the microscope by a beam splitter (OCT-21020-BX3TRF) and focused to a spot size of ∼425 nm by a 40X/1.3 numerical aperture (NA) oil immersion objective lens (Olympus, Tokyo, Japan). A coverslip is positioned just before the beam splitter to divert ∼2% of the laser beam onto a power meter that has been precisely calibrated to determine the average power at the sample stage. The condenser lens (Nikon, Tokyo, Japan) collects the forward scattered light and redirects it into the beam splitter such that the light can be focused
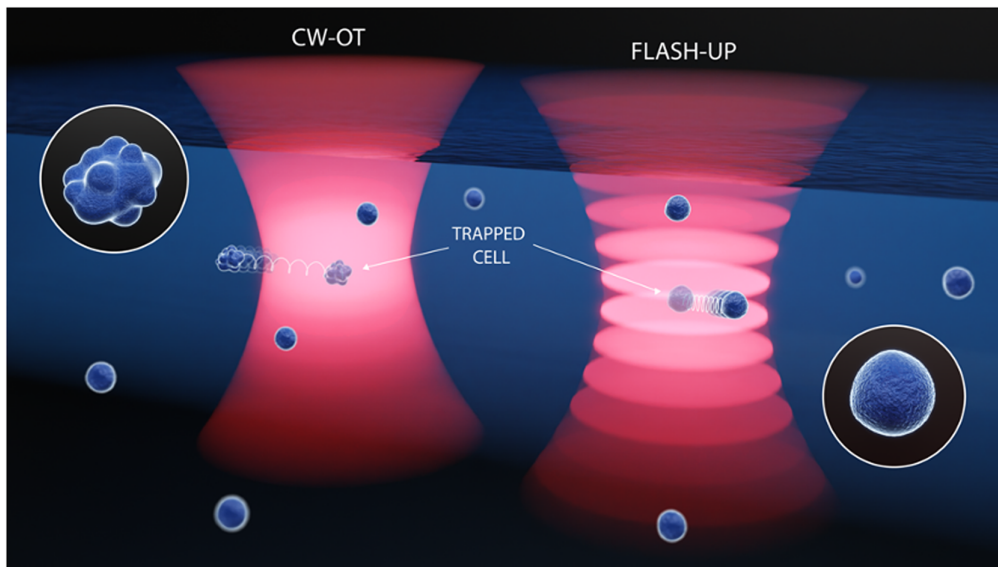
Fig. 1 Concept art highlighting optical trapping using CW and FLASH-UP. Conventional CW (left) and fs (right) lasers optically trapping cells in an aqueous environment. A cell after being trapped with the CW laser has undergone potential deformations and/or damaged secreted adhesion proteins adversely affecting cell motility, whereas a cell trapped by FLASH-UP retains its motility functions and experiences a stronger optical force.
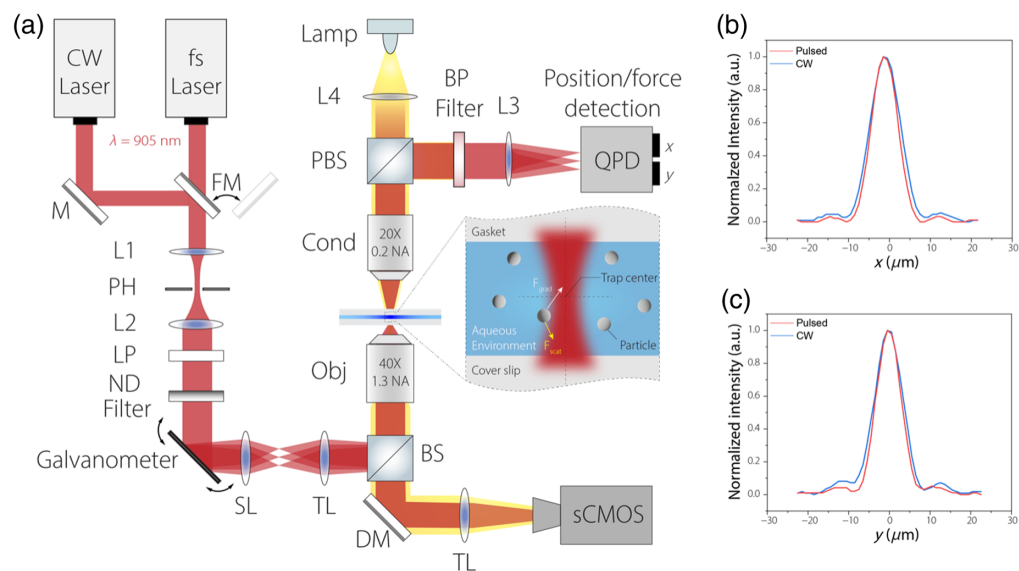

Fig. 2 (a) CW or pulsed laser source is employed for optical trapping of particles. L, lens; M, mirror; FM, flip mirror; DM, dichroic mirror; PH, pinhole; LP, linear polarizer; ND, neutral density; SL, scanning lens; TL, tube lens; BS, beam splitter; PBS, polarizing beam splitter; BP, bandpass filter; QPD, quadrant photodiode. (b) Horizontal and (c) vertical line profiles of pulsed and CW lasers.

into the quadrant photodiode (QPD; Thorlabs, PD80A, Newton, New Jersey, United States) by a lens. The x and y voltage outputs from the QPD are recorded using an oscilloscope (PicoScope, 3203D, Tyler, Texas, United States) from which the trap stiffness, κ, is extrapolated via the power spectrum method found in Eq. (S2) in the Supplementary Material. Visualization of the sample is enabled by a 150-W halogen fiber optical light source (AmScope, HL150-AY, Irvine, California, United States), and time-lapse sequences are imaged with an scientific complementary metal-oxide sensor (sCMOS) (Hamamatsu, C15440-20UP, Hamamatsu, Japan). Line profiles of both lasers are compared and displayed in Figs. 2(b) and 2(c) at $z = 0$ μm, demonstrating negligible differences.
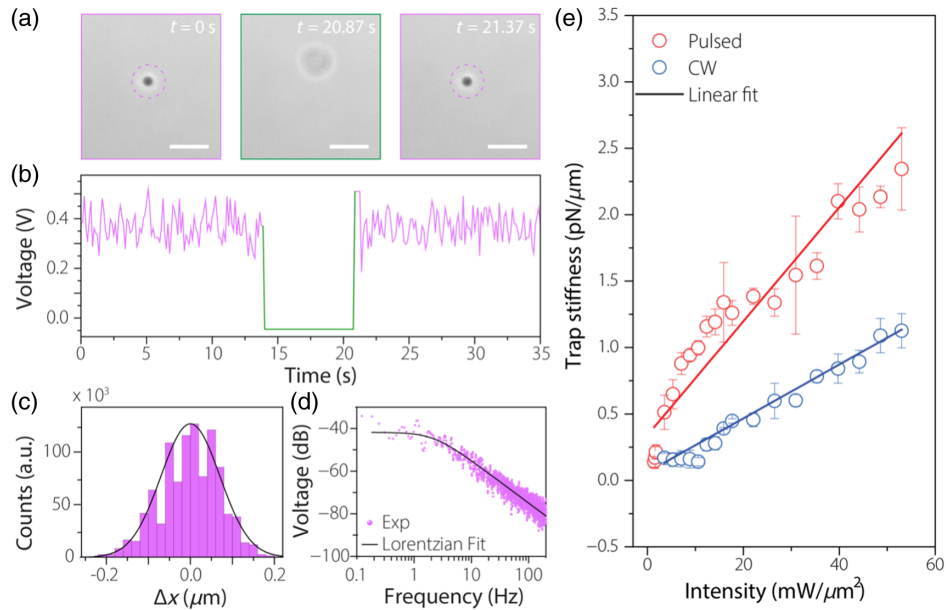
Fig. 3 (a) Time-lapse sequence of a silica microsphere in (magenta) and out (green) of a trap when the laser is on/off (Video 1). The dotted circles represent the laser position. (b) Corresponding voltage output versus time relating to particle position. (c) 1D position histogram of particles within the trap. (d) Fitting of single-sided Lorenzian to extrapolate the corner frequency. (e) Trap stiffness dependence on input intensity for pulsed (d) and CW (blue) lasers. Data is presented as mean values ± SD of the mean. Scale bars, 5 μm. (Video 1, MP4, 156 KB [URL: https://doi.org/10.1117/1.JBO.29.8.086501.s1]).

4 Results

4.1 Observation of Ultra-Low-Power Optical Trapping of Dielectric Spheres

Output voltages are recorded from a QPD when a particle is trapped. Minimal trapping thresholds I_{thr} and trapping efficiencies $Q = Fc/nP$, where F, c, n, and P are the force exerted on the particle, speed of light, particle refractive index, and average power, respectively, are determined for a range of average intensities from 1.41 mW/μm^2 ($P = 80\ \mu$W) to 17.67 mW/μm^2 ($P = 1$ mW). Figure 3(a) depicts a trapped microsphere (magenta frame) with the fs laser source at time $t = 0$ s. When the trap is turned off at $t = 20.87$ s, the particle is released from the trap and is no longer within the trapping plane (green). However, when the laser is reactivated at $t = 21.37$ s, the particle returns to its initial trapped position (magenta) and remains trapped for the remainder of the experiment ($t = 35$ s). The corresponding voltage displacement collected by the QPD is shown in Fig. 3(b). The particle is confined to a harmonic potential well [Fig. 3(c)], and the κ is rendered by fitting the power spectrum to a single-sided Lorenzian [Fig. 3(d)].

Figure 3(e) depicts the trap stiffness of FLASH-UP (red) and CW (blue) lasers for the microspheres (Video 1). The experiment is conducted on three different particles, and values are given as mean $\pm$ standard deviation (SD). The values of I_{thr} for FLASH-UP and CW lasers are 1.41 and 3.51 mW/μm^2, respectively. Trap stiffness κ ranges from 0.30 to 2.82 pN/μm for pulsed and 0.25 to 0.55 pN/μm for CW. To quantitatively evaluate the trap strength, we apply a fit (slope = η) that matches well with experimental data. We find that FLASH-UP not only has $\eta = 0.14$ pN $\cdot\ \mu$m $\cdot$ mW^{-1}, whereas CW has $\eta = 0.025$ pN $\cdot\ \mu$m $\cdot$ mW^{-1}, but also stably traps a single particle at a lower intensity threshold.

4.2 Trapping Bacterial Cells

To investigate the use of FLASH-UP for biological applications, we perform OT experiments on bacterial cells. We select four differently shaped pathogenic bacteria, namely, *S. aureus* (spherical), *B. paranthracis* (rod), *V. cholerae* (jellybean), and *S. epidermidis* (elliptical). The morphological characterization of each cell is given in Fig. S1 in the Supplementary Material. The average aspect ratios and areas of *S. aureus* are 1.21 and 0.40 μm^2, *B. paranthracis*
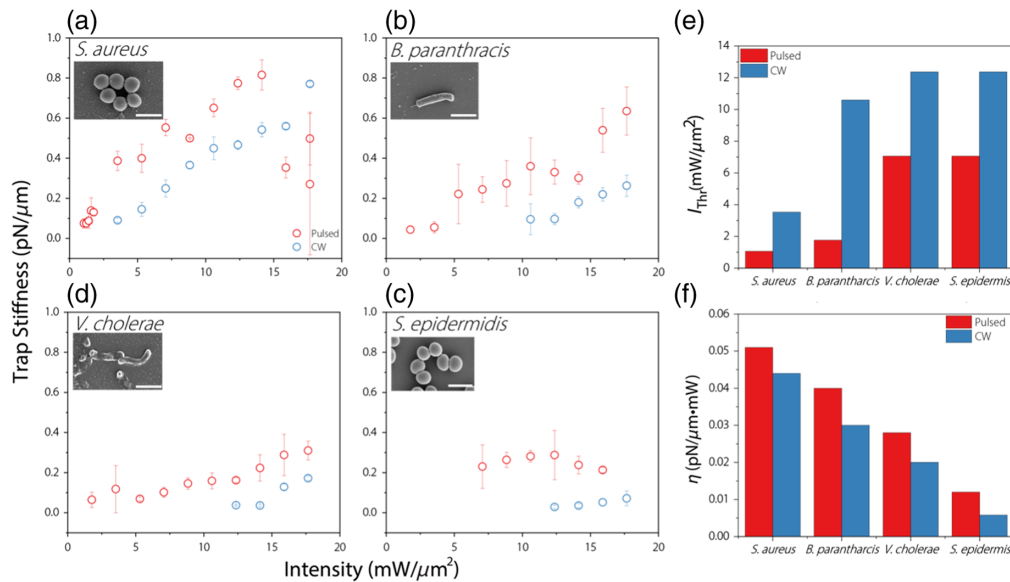
Fig. 4 Comparing trap stiffness (mean ± SD) for pulsed (red) and CW (blue) lasers based on intensity for (a) *S. aureus*, (b) *B. paranthracis*, (c) *S. epidermidis*, and (d) *V. cholerae*. (e) Threshold intensities required for trapping each cell. (f) Trap efficiencies for each cell. Scale bars, 5 μm.

are 3.01 and 2.04 μm^2, *V. cholerae* are 2.28 and 1.10 μm^2, and *S. epidermidis* are 1.26 and 0.37 μm^2, respectively.

Trap stiffnesses are determined as described in the Sec. 4.1. Figures 4(a)–4(d) display the trap stiffness of each cell type for both pulsed (red) and CW (blue) lasers. The insets of each graph are scanning electron microscopy (SEM) images obtained for each bacteria type. We find that FLASH-UP demonstrates a stronger trap stiffness for each cell type compared with using a CW source. The I_{thr} for each cell is shown in Fig. 4(e). Moreover, the η shown in Fig. 4(f) depicts that the trap stiffness using FLASH-UP consistently exhibits a higher stiffness than CW regardless of bacteria type. Interestingly, this intensity may go down even lower depending on the trapping media used due to differences in refractive indices and thermal properties, changing the trapping conditions.[35,36] In Fig. S2 in the Supplementary Material, we measured the trap stiffness of silica microspheres in deionized (DI) water and 1× phosphate buffer saline (PBS) of both laser sources. We observed that the trap stiffness of the dielectrics for both lasers in 1× PBS was lower than in DI water at intensities above 1.76 mW/μm^2 for FLASH-UP and 7.06 mW/μm^2 for CW.

To understand the effects of the lasers on cell motility, we conduct an experiment whereby *S. aureus* cells are trapped by either laser for 90 s at intensities of 8.83 mW/μm^2. Subsequently, the laser is turned off (effectively turning off the trap), and time-lapse image sequences are captured at a time resolution of 5 μs with the cell position over 60 s being assessed using ImageJ (Fig. 6 in the Appendix). Interestingly, we note that *S. aureus* cells are immobilized after they were briefly trapped by the CW laser (blue; Video 2). However, this is not observed with FLASH-UP (red; Video 3). As a control, we also plot the Brownian motion of a cell that was not trapped (gray; Video 4). It is evident that there is minimal movement of the cell once it is released from the trap by the CW laser source as the SD of the cell position is 2× lower than FLASH-UP and the control.

Figure 5(a) depicts the trap stiffness of *P. aeruginosa* for FLASH-UP (red) and CW (blue) lasers. Morphology characterization is given in Fig. S1 in the Supplementary Material, and the average aspect ratio and area are 2.30 and 0.64 μm^2, respectively. The I_{thr} for trapping these cells are 1.76 mW/μm^2 and 7.06 mW/μm^2 for the pulsed and CW sources, respectively. FLASH-UP also exhibits a stiffer trap for all intensities compared with the CW.

After the cell is trapped with either laser, we turn off the trap and track the cell position similarly demonstrated in Fig. 6 in the Appendix. We then plot the trajectory of the cells along the *x-y* plane with respect to time (denoted from magenta to teal) for 5 s for pulsed (top) and CW (bottom) sources in Fig. 5(b). It is observed that the cell has a longer trajectory after being released from FLASH-UP (Video 5). However, the swimmer cell remains immobilized within the trap region after it has been released from the CW source (Video 6). Using ImageJ, the

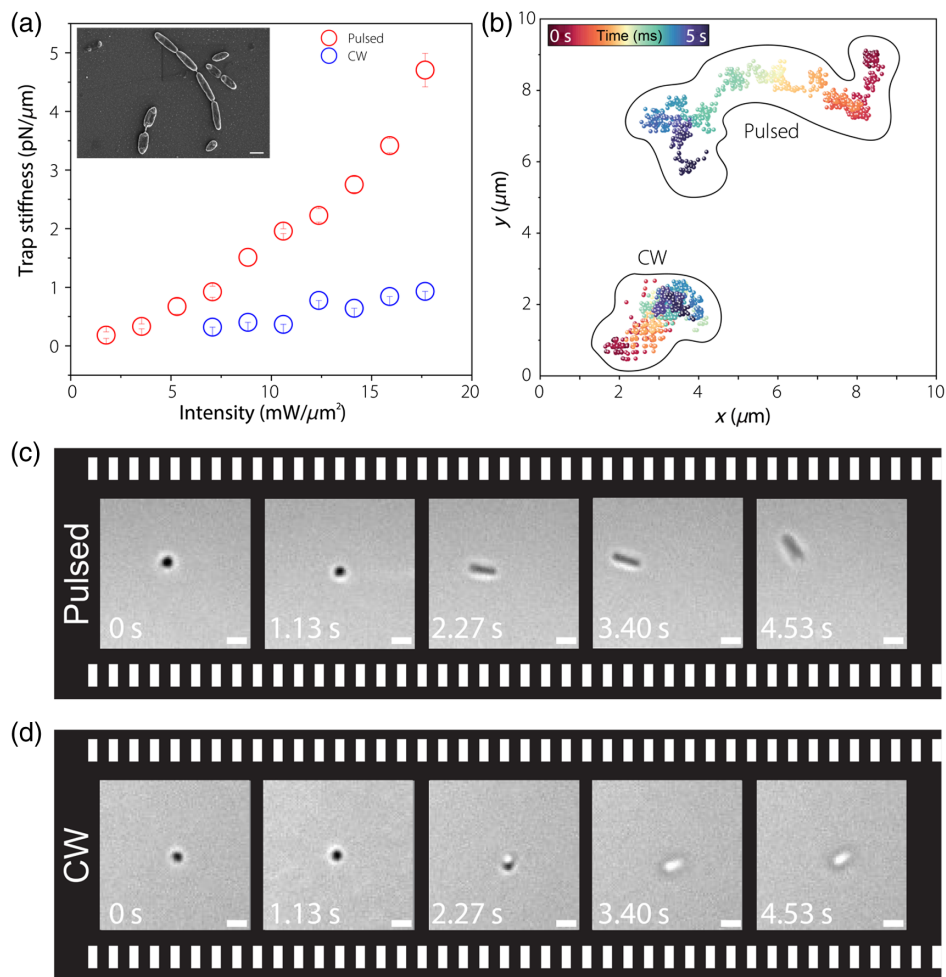**Fig. 5** (a) Comparing trap stiffness (mean ±. SD) of pulsed (red) and CW (blue) based on intensity for *P. aeruginosa*. (b) Cell trajectory with respect to time after being trapped for 5 s. Time-lapse sequence of a cell once the trap is turned off for (c) pulsed (Video 5) and (d) CW (Video 6). Scale bars, 1 μm. (Video 5, MP4, 76 KB [URL: https://doi.org/10.1117/1.JBO.29.8.086501.s5]; Video 6, MP4, 76 KB [URL: https://doi.org/10.1117/1.JBO.29.8.086501.s6]).

displacement of the cell from the trap position is calculated yielding 4.4 μm for pulsed and 1.35 μm for CW. Moreover, the cell after being trapped by FLASH-UP is nearly 2 mm longer than the CW. Figures 5(c) and 5(d) represent a time-lapse sequence of the cells after they have been trapped for 5 s by the pulsed and CW lasers, respectively.

5 Discussion and Conclusion

We experimentally demonstrate for the first time that, under specific conditions, OT using FLASH-UP significantly outperforms conventional OT (by a five-fold improvement in trap stiffness), thereby enabling the direct manipulation of cells with ultra-low average power OT. Importantly, although conventional OT using a CW source has been around for more than 50 years and trapping with a pulsed source for at least 30 years, we found a regime that has heretofore been overlooked by researchers in the field: the specific intersection of ultra-low average powers on the order of tens of microwatts (corresponding to intensities as low as 1.4 mW/μm^2) and particles in the Lorenz–Mie (intermediate) regime, a regime that is relevant for cells, yields incredibly stiff traps.

A careful review of the OT literature reveals that there are apparently conflicting conclusions regarding the advantages of pulsed versus CW OT. Upon inspection, one will find that a significant reason for the apparent conflict is that the conditions of comparison for the OT experiments are often not the same. Quite often, researchers explore OT in the few milliwatts to hundreds of milliwatt power regimes, and for some, the focus is on Rayleigh particles, whereas

for others, it is on much larger Mie particles. This is important as the OT energy landscape is influenced by many experimental parameters, including power, particle size, type, and material. Thus, under specific conditions, the distinction between pulsed and CW has been inconclusive, and for other conditions, one will find that one type of OT outperforms the other. In our case, we are exploring a region that has not been explored and is significant because of its particular utility to biophysics. Although the underlying mechanism is still an area of investigation (and we attribute it to a transient force), our experimental results are incontrovertible. One may posit that the enhancement in trap stiffness for FLASH-UP stems from the nonlinear effects of trapping. This assertion might be applicable when trapping metallic nanoparticles under high average power conditions, typically on the order of hundreds of milliwatts. These particles have demonstrated their ability to function as local antennas, augmenting light–matter interaction. Consequently, they facilitate the emergence of specific nonlinear effects such as the amplification of the imaginary component of $\chi^{(3)}$.[37,38] Nevertheless, our investigation operates within a regime in which nonlinear effects are not anticipated below a specific fluence threshold, especially for dielectric particles and bacteria.

Our work is extremely significant as we show unambiguously the direct (i.e., without the use of functionalized spheres as a handle) optical trapping of cells without any observable deleterious effects on cell motility, in contrast to using a CW laser with the same intensity and wavelength as the control experiment. This paves the way for enhanced cell retention over extended durations, opening avenues for investigating dynamic biological processes such as gene expression and protein localization during cell division. This capability extends to seamlessly transporting cells across diverse channels with varying compositions and conducting diagnostic mechanical testing at the cellular level. Specifically, leveraging the potential of FLASH-UP for ultra-low-power trapping of bacteria holds promise for the in-depth exploration of microbial adhesion, bacterial surface colonization, and the formation of biofilms. Employing OT allows for the precise manipulation of bacterial spacing, facilitating a comprehensive understanding of how cell density influences cell-to-cell signaling. Furthermore, aligning bacteria with each other provides valuable insights into their preferred growth directions. FLASH-UP potentially could be used not only to deepen comprehension of biofilm formation, a common occurrence on medical implants, surgical fixations, and vascular replacements, but also to advance our knowledge in manipulating cellular behavior for biomedical applications.

6 Appendix

Cells were trapped with either laser for 90s at intensities of 8.83 mW/μm^2. After the trap was turned off, cell positions were assessed over 60s. We note that the cell after being released with the CW laser was immobilized, which was otherwise not seen in the control and FLASH-UP.
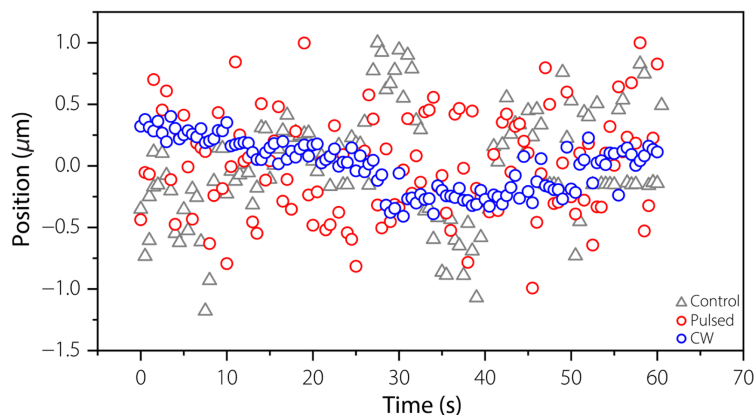

Fig. 6 After cells have been released from the traps by CW (blue; Video 2), and pulsed (red; Video 3), the positions of the cells are tracked after the trap has been turned off. Control (grey; Video 4) is represented as the Brownian motion of a cell when it has not been exposed to any lasers. (Video 2, MP4, 152 KB [URL: https://doi.org/10.1117/1.JBO.29.8.086501.s2]; Video 3, MP4, 315 KB [URL: https://doi.org/10.1117/1.JBO.29.8.086501.s3]; Video 4, MP4, 86 KB [URL: https://doi.org/10.1117/1.JBO.29.8.086501.s4]).

Disclosures

The authors declare no conflicts of interest.

Code and Data Availability

All data needed to evaluate the conclusions in the paper are present in the paper and/or the Supplementary Material. Additional data related to this paper may be requested from the authors.

Acknowledgments

References

1. A. Ashkin and J. M. Dziedzic, "Optical levitation by radiation pressure," *Appl. Phys. Lett.* **19**(8), 283–285 (2003).
2. V. P. Oleshko and J. M. Howe, "Chapter three—electron tweezers as a tool for high-precision manipulation of nanoobjects," in *Advances in Imaging and Electron Physics*, P. W. Hawkes, Ed., Vol. **179**, p. 203–262, Elsevier (2013).
3. A. Ashkin, "Acceleration and trapping of particles by radiation pressure," *Phys. Rev. Lett.* **24**(4), 156–159 (1970).
4. K. Dholakia and P. Reece, "Optical micromanipulation takes hold," *Nano Today* **1**(1), 18–27 (2006).
5. A. Ashkin, J. M. Dziedzic, and T. Yamane, "Optical trapping and manipulation of single cells using infrared laser beams," *Nature* **330**(6150), 769–771 (1987).
6. K. C. Neuman and S. M. Block, "Optical trapping," *Rev. Sci. Instrum.* **75**(9), 2787–2809 (2004).
7. M. Pradhan et al., "Optically trapping tumor cells to assess differentiation and prognosis of cancers," *Biomed. Opt. Express* **7**(3), 943–948 (2016).
8. S. Hu et al., "Advanced optical tweezers on cell manipulation and analysis," *Eur. Phys. J. Plus.* **137**(9), 1024 (2022).
9. M. Waleed et al., "Single-cell optoporation and transfection using femtosecond laser and optical tweezers," *Biomed. Opt. Express* **4**(9), 1533–1547 (2013).
10. F. Schlosser, F. Rehfeldt, and C. F. Schmidt, "Force fluctuations in three-dimensional suspended fibroblasts," *Philos. Trans. R. Soc. B. Biol. Sci.* **370**(1661), 20140028 (2015).
11. N. Rezaei et al., "Using optical tweezers to study mechanical properties of collagen," *Proc. SPIE* **8007**, 80070K (2011).
12. C. Bustamante, Z. Bryant, and S. B. Smith, "Ten years of tension: single-molecule DNA mechanics," *Nature* **421**(6921), 423–427 (2003).
13. K. Svoboda and S. M. Block, "Optical trapping of metallic Rayleigh particles," *Opt. Lett.* **19**(13), 930–932 (1994).
14. A. Blázquez-Castro, "Optical tweezers: phototoxicity and thermal stress in cells and biomolecules," *Micromachines* **10**(8), 507 (2019).
15. N. Malagnino et al., "Measurements of trapping efficiency and stiffness in optical tweezers," *Opt. Commun.* **214**(1), 15–24 (2002).
16. G. Honglian et al., "Measurements of displacement and trapping force on micron-sized particles in optical tweezers system," *Sci. China Ser. A-Math.* **45**(7), 919–925 (2002).
17. J. Kim and J. H. Shin, "Stable, free-space optical trapping and manipulation of sub-micron particles in an integrated microfluidic chip," *Sci. Rep.* **6**(1), 33842 (2006).
18. K. Krishna et al., "Using flat-top light sheet generated by femtosecond-pulsed laser for optical manipulation of microscopic particles," *Proc. SPIE* **12649**, 126490L (2023).
19. C. Zhao, "Practical guide to the realization of a convertible optical trapping system," *Opt. Express* **25**(3), 2496–2510 (2017).
20. F. Català et al., "Influence of experimental parameters on the laser heating of an optical trap," *Sci. Rep.* **7**(1), 16052 (2017).
21. S. P. Gross, "Application of optical traps in vivo," *Methods Enzymol.* **361**, 162–174 (2003).

22. J. Li et al., "Opto-refrigerative tweezers," *Sci. Adv.* **7**(26), eabh1101 (2021).

23. J. Zhou et al., "Low-temperature optothermal nanotweezers," *Nano. Res.* **16**(5), 7710–7715 (2023).

24. K. R. Peddireddy et al., "Optical-tweezers-integrating-differential-dynamic-microscopy maps the spatiotemporal propagation of nonlinear strains in polymer blends and composites," *Nat. Commun.* **13**(1), 5180 (2022).

25. M. D. Wang et al., "Stretching DNA with optical tweezers," *Biophys. J.* **72**(3), 1335–1346 (1997).

26. S. Ayano et al., "Quantitative measurement of damage caused by 1064-nm wavelength optical trapping of *Escherichia coli* cells using on-chip single cell cultivation system," *Biochem. Biophys. Res. Commun.* **350**(3), 678–684 (2006).

27. T. Shoji et al., "Permanent fixing or reversible trapping and release of DNA micropatterns on a gold nanostructure using continuous-wave or femtosecond-pulsed near-infrared laser light," *J. Am. Chem. Soc.* **135**(17), 6643–6648 (2013).

28. J. Gong, F. Li, and Q. Xing, "Femtosecond optical trapping of cells: efficiency and viability," *Trans. Tianjin Univ.* **15**(5), 315–318 (2009).

29. D. Goswami, "Understanding femtosecond optical tweezers: the critical role of nonlinear interactions," *J. Phys. Conf. Ser.* **1919**(1), 12013 (2021).

30. A. K. De et al., "Stable optical trapping of latex nanoparticles with ultrashort pulsed illumination," *Appl. Opt.* **48**(31), G33–G37 (2009).

31. K. B. Im et al., "Trapping efficiency of a femtosecond laser and damage thresholds for biological cells," *J. Korean Phys. Soc.* **48**, 968–973 (2006).

32. B. Agate et al., "Femtosecond optical tweezers for in-situ control of two-photon fluorescence," *Opt. Express* **12**, 3011–3017 (2004).

33. A. Singh et al. "Experimental comparison of conventional and femtosecond optical tweezers," in *Conf. Lasers Electro-Opt., OSA Tech. Digest*, Optica Publishing Group, p. JW1A.153 (2021).

34. D. P. G. Nilsson et al., "Physico-chemical characterization of single bacteria and spores using optical tweezers," *Res. Microbiol.* **174**(6), 104060 (2023).

35. L. G. Wang and C. L. Zhao, "Dynamic radiation force of a pulsed Gaussian beam acting on Rayleigh dielectric sphere," *Opt. Express* **15**(17), 10615–10621 (2007).

36. B. J. Roxworthy et al., "Plasmonic optical trapping in biologically relevant media," *PLoS One* **9**(4), e93929 (2014).

37. Y. Qin et al., "Nonlinearity-induced nanoparticle circumgyration at sub-diffraction scale," *Nat. Commun.* **12**, 3722 (2021).

38. L. Huang et al., "Spheroidal trap shell beyond diffraction limit induced by nonlinear effects in femtosecond laser trapping," *Nanophotonics* **9**(14), 4315–4325 (2020).

39. K. Berg-Sørensen and H. Flyvbjerg, "Power spectrum analysis for optical tweezers," *Rev. Sci. Instrum.* **75**(3), 594–612 (2004).

Krishangi Krishna received her BE degree in biomedical engineering from Stony Brook University in 2019. She is currently a PhD candidate in the PROBE lab in the School of Engineering at Brown University. Her research interests lie in optical tweezers, plasmonics, ultrafast optics, and imaging modalities.

Joshua A. Burrow received his BS degree in mathematics and physics from Morehouse College in 2012. He earned his MS degree and PhD from the Electro-Optics Department at the University of Dayton in 2017 and 2021, respectively. He joined the School of Engineering at Brown University as a Hibbitt postdoctoral fellow and is currently a Burroughs Wellcome Fund fellow in the PROBE Lab. His research interests are in active linear and nonlinear light–matter interactions, polarization microscopy, and biophotonics.

Zhaowei Jiang received her BS and MS degrees from Syracuse University. She is currently a PhD candidate in the Shukla Laboratory for Designer Biomaterials at Brown University. Her research interests are in developing nanomaterials for the treatment of bacterial infections.

Wenyu Liu is currently an undergraduate student of engineering physics and applied math at Brown University. His research interests at the PROBE Lab include ultrafast optical tweezers, Hong-Ou-Mandel interferometry, and quantum–quantum-induced coherence imaging.

Anita Shukla is the Elaine I. Savage Associate Professor of Engineering and a member of the Center for Biomedical Engineering at Brown University. Her research focuses on designing responsive and targeted biomaterials for applications in drug delivery and regenerative medicine.

Kimani C. Toussaint, Jr., is the Thomas J. Watson, Sr. Professor in the School of Engineering at Brown University. He is the senior associate dean in the School of Engineering and director of the Brown–Lifespan Center for Digital Health. He directs the laboratory for Photonics Research of Bio/Nano Environments, an interdisciplinary research group focusing on developing nonlinear optical imaging techniques for the quantitative assessment of biological tissues and novel methods for harnessing plasmonic nanostructures for light-driven control of matter.